

# Controllable unidirectional transport and photon storage in an one-dimensional lattice with complex hopping rates

Lei Du<sup>†</sup> and Yan Zhang

Center for Quantum Sciences and School of Physics,  
Northeast Normal University, Changchun 130117, P. R. China and

<sup>†</sup>leiduphys@outlook.com

(Dated: December 3, 2024)

We study an one-dimensional non-Hermitian lattice with complex hopping rates, which can be realized by a quasi-one-dimensional sawtooth-type Hermitian lattice after adiabatic elimination with proper conditions. By means of synthetic magnetic fluxes, the imaginary parts of the complex hopping rates can be modulated by additional phase, thus a non-reciprocal structure arises. With this lattice, one can realize robust unidirectional transport for both single-site and Gaussian excitations, which is immune to defects and backscattering. Furthermore, we proposed a sandwich structure based on the non-Hermitian lattice, which can be used for realizing controllable photon storage and reversal. The storage time and range can be artificially controlled within limits, and the storage efficiency can be increased via a finite gain compensation. The proposal of controllable photon transport in this paper opens up a new path for unidirectional photon transport and provides a promising platform for optical control and manipulation.

PACS numbers: 42.50.-p, 42.50.Pq, 42.65.-k

## I. INTRODUCTION

The realization of controllable and directional photon transport is vital for a large variety of areas and has been a major goal of research for decades. Especially, unidirectional photon transport, which can be used for realizing optical isolators and diodes, plays a key role in modern optics. Generally, unidirectional wave transport can be observed in an asymmetric hybrid system in which a nonlinear system is embedded in a linear medium [1–3], or a two-(three-)dimensional photonics system with topological protection [4–6]. As is well-known, topologically protected edge states, which are guided by synthetic gauge fields and propagate at the boundary of the samples, have exhibited enormous advantages due to the robustness, i.e., they are immune to disorders and scattering. However, such schemes are realized only in two- or three-dimensional photonics systems such as quantum Hall systems, topological insulators and topological superconductors, rather than one-dimensional photonics lattice.

An alternative platform for realizing controllable and directional photon transport is the non-Hermitian photonic lattice, in which a large amount of important phenomena have been observed, such as non-Hermitian delocalization in disorder lattices [7–14], invisible defects [15], topological phase transitions [16–18], non-Hermitian induced flat bands [19–21], invisible non-Hermitian optical potentials [22, 23] and so on. Recently, inspired by the non-Hermitian delocalization proposed by Hatano and Nelson [7], a scheme of realizing robust unidirectional photon transport in one-dimensional non-Hermitian lattice was proposed by Longhi *et al.* [24, 25]. In those works, an imaginary gauge field, which can be acquired by exploiting auxiliary ring resonators with gain and loss in different half perimeters respectively, leads to a non-

reciprocal hopping rates. By means of the imaginary gauge field, the wave propagates in one direction is amplified, whereas it is attenuated in the opposite direction. Thus an unidirectional transport arises. Subsequently, a non-Hermitian lattice with imaginary hopping rates, which can be used for realizing robust bidirectional photon transport, is proposed in Refs. [26, 27]. These inspiring works enable non-Hermitian lattices to be feasible and excellent platforms for robust directional photon transport.

In this paper, we show that a class of one-dimensional non-Hermitian lattices, with complex hopping rates whose imaginary parts are modulated by synthetic magnetic fluxes. Such a non-Hermitian can be realized by a tailored quasi-one-dimensional sawtooth-type Hermitian lattice with adiabatic elimination. In the non-Hermitian lattice, robust unidirectional photon transport can be observed which is immune to defects and backscattering. Furthermore, we also show a sandwich structure, i.e., a three-stage heterogeneous structure, can be utilizing as a photon storer. By modulating relevant parameters, one can realize both photon storage and reversal. The storage time and range can be artificially controlled within limits, and the storage efficiency can be increased by a gain compensation in finite lattice sites.

## II. MODEL AND EQUATIONS

We consider photon transport in a quasi-one-dimensional sawtooth-type lattice, consisting of a main sublattice  $A$  with optical potential  $U_{a,n}$  and Wannier state  $|n\rangle_A$ , and an auxiliary sublattice  $B$  with optical potential  $U_{b,n}$  and Wannier state  $|n\rangle_B$ , at the  $n$ th sites of  $A$  and  $B$ , as schematically shown in Fig. 1 (a). As in general optical lattices, the real

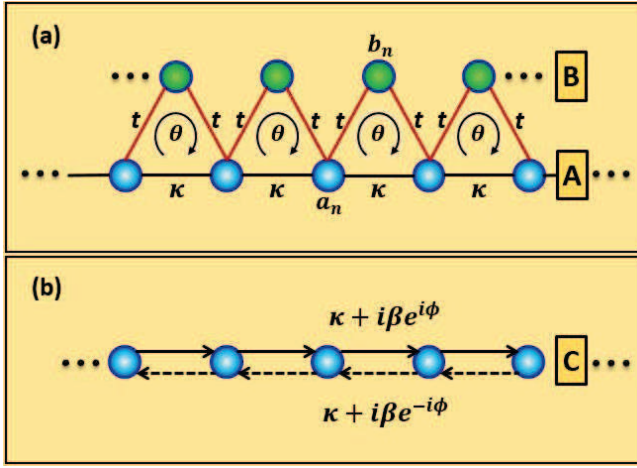


FIG. 1: (Color online) Schematic illustration of (a) the quasi-one-dimensional sawtooth-type lattice which serves as the physical realization of the non-Hermitian lattice proposed in this paper and (b) the equivalent one-dimensional non-Hermitian Lattice with complex hopping rates whose imaginary parts are modulated by synthetic magnetic fluxes. Here,  $\kappa$  is the hopping rate between adjacent sites on the sublattice A and  $t$  is the hopping rate between the nearest-neighbor sites on the sublattices A and B, respectively.

parts of potentials  $V_{a(b)} = \text{Re}[U_{a(b)}]$  denote detunings (coupled-resonator systems) or propagation constants (optical-waveguide systems), and the imaginary parts  $\gamma_{a(b)} = \text{Im}[U_{a(b)}]$  denote gain or loss effects. Hereafter, we assume a uniform imaginary part  $\gamma$  for the whole sublattice A, corresponding to a homogeneous loss rate. Indicating by  $a_n$  and  $b_n$  the probability amplitudes of the  $n$ th sites of sublattices A and B, the evolution equations of the system in the tight-binding approximation can be written as

$$\begin{aligned} i \frac{da_n}{dt} &= U_{a,n} a_n + \kappa(a_{n+1} + a_{n-1}) + t(e^{i\theta} b_n + e^{-i\theta} b_{n-1}) \\ i \frac{db_n}{dt} &= U_{b,n} b_n + t(e^{i\theta} a_{n+1} + e^{-i\theta} a_n) \end{aligned} \quad (1)$$

where  $\kappa$  is the hopping rate between the nearest-neighbor sites on sublattice A and  $t$  is the nearest-neighbor hopping rate between sites on sublattices A and B, respectively. We set  $\theta$  the synthetic magnetic fluxes perpendicular to the plane of the quasi-one-dimensional lattice, which can be acquired by exploiting synthetic gauge fields [27–29]. A simple and feasible scheme for generating effective magnetic fields by means of optomechanics on a lattice is proposed [29]. Moreover, synthetic magnetic fluxes can also be introduced by optical path imbalances between sites [28] or modulated on-site potentials [30]. By assuming a uniform optical potential  $U_b$ , the auxiliary sublattice B can be eliminated adiabatically, i.e.,

$$b_n \simeq \frac{-t[e^{i\theta} a_{n+1} + e^{-i\theta} a_n]}{U_b} \quad (2)$$

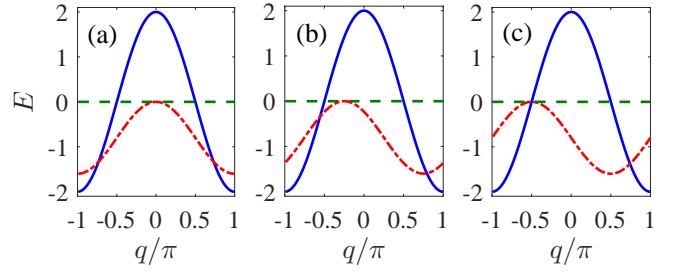


FIG. 2: (Color online) The real part (blue solid line) and the imaginary part (red dot-dashed line) of the energy dispersion curve versus the Bloch wave number  $q$  with (a)  $\phi = 0$ ; (b)  $\phi = \pi/4$ ; (c)  $\phi = \pi/2$ . The green dashed line denotes  $E = 0$  as a reference line. Other parameters are  $\gamma = 0.8\kappa$  and  $\beta = 0.4\kappa$ . The energy scale is in arbitrary units.

if  $|U_b|$  is much larger than  $t$  and energy  $E$  (in modulus) of the system ( $-2\kappa \leq |E| \leq 2\kappa$ ) [26, 27]. Then the equivalent evolution equations can be read

$$i \frac{da_n}{dt} = U_{eff,n} a_n + J_1 a_{n+1} + J_2 a_{n-1} \quad (3)$$

where  $U_{eff,n} = U_{a,n} - 2t^2/U_b$  denotes the effective optical potential at the  $n$ th site,  $J_1 = \kappa - t^2 e^{2i\theta}/U_b$  and  $J_2 = \kappa - t^2 e^{-2i\theta}/U_b$  denote the non-reciprocal effective hopping rates between adjacent sites of sublattice A, after the adiabatical elimination, respectively. Note, equivalent complex hopping rates  $\kappa + i\beta e^{\pm 2i\theta}$ , which the imaginary parts are modulated by synthetic magnetic fluxes, are generated if  $U_b = it^2/\beta$ . It is so different from the general Hermitian lattices where the hopping rates are real and this will be discussed in the next section. In view of this, we can introduce an equivalent one-dimensional lattice C with complex hopping rates, as shown in Fig. 1 (b). The evolution equations of the non-Hermitian lattice C can be written as

$$i \frac{dc_n}{dt} = -i\gamma c_n + (\kappa + i\beta e^{i\phi}) c_{n+1} + (\kappa + i\beta e^{-i\phi}) c_{n-1} \quad (4)$$

with  $\phi = 2\theta$ . Here, we have removed the real parts of  $U_{eff}$  by setting  $V_a = 2t^2/U_b$ , because a nonvanishing real part only shifts the dispersion relation. Such a set of coupled evolution equations describe the dynamics of the non-Hermitian lattice with complex hopping rates whose imaginary parts are modulated by an additional Peierls phase  $\phi$  due to the synthetic magnetic fluxes. The phase  $\phi$  can be precisely adjusted in several implementation schemes mentioned above, it seems that a phase-dependent control of light propagation can be realized.

By setting the solutions to Eq. (3) in form  $c_n = C \exp(iqn - iEt)$ , the dispersion relation of this lattice can be written as

$$E(q) = 2\kappa \cos(q) + 2i\beta \cos(q + \phi) - i\gamma \quad (5)$$

with  $-\pi \leq q \leq \pi$  is the Bloch wave number (quasi-momentum) in the first Brillouin zone. One can find

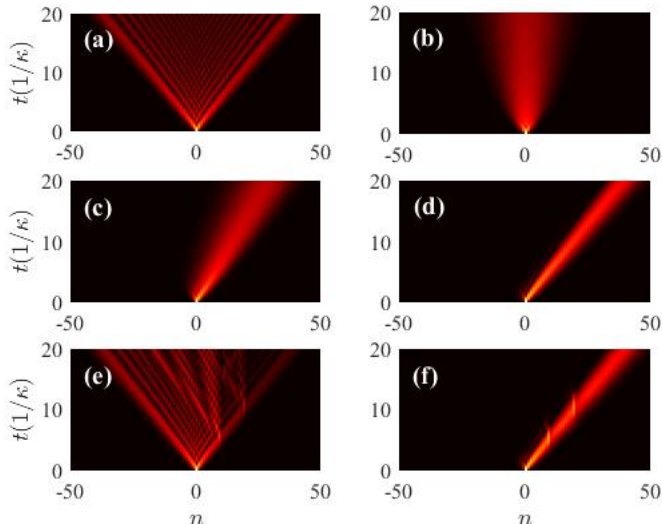


FIG. 3: (Color online) Dynamics of wave propagation in Hermitian and non-Hermitian lattices with single-site excitation at initial time. We plot in figures the space-time evolution of the normalized probability amplitude  $|\rho_n(t)|$  in Hermitian lattices without [(a)] and with [(e)] defects, non-Hermitian lattices without [(b)-(d)] and with [(f)] defects. We set  $\gamma = \beta = 0$  in the Hermitian case and  $\beta = 0.4\kappa, \gamma = 0.8\kappa$  in the non-Hermitian case. The lattice defects are assumed to be  $V_c = 2\kappa$  at  $n = 10, 20$ . Other parameters are (b)  $\phi = 0$ , (c)  $\phi = \pi/4$ , (d) and (f)  $\phi = \pi/2$ . In the Hermitian case the dynamics do not depend on the phase  $\phi$ .

that the imaginary part of the dispersion relation which describes the amplification or absorption effect, can be modified by the phase  $\phi$ , while the real part which determines the group velocity, i.e.,

$$v_g = \text{Re}(dE/dq) = -2\kappa \sin(q) \quad (6)$$

is invariable with  $\phi$ . Note that a purely dissipative optical system requires  $\gamma \geq 2\beta$  [27]. Moreover, we point out that a Hermitian lattice arises when  $\gamma = \beta = 0$ .

We show in Fig. 2 the dispersion curve as the function of  $q$ . As predicted by Eq. (4), the position of imaginary part of the dispersion relation (especially the maximal value  $\text{Im}(E)_{max} = 0$  which means a lossless light propagation) can be changed by adjusting the phase  $\phi$  while the real part keeps invariable.

### III. ROBUST UNIDIRECTIONAL PHOTON TRANSPORT

We first consider wave propagation in the non-Hermitian lattice  $C$  with single-site excitation at initial time  $t = 0$ , i.e.,  $c_n(0) = \delta_{n,0}$ . Fig. 3 shows numerically the space-time evolution of the normalized probability amplitude  $\rho_n(t)$ ,

$$\rho_n(t) = \sqrt{\frac{|c_n(t)|^2}{S(t)}}, \quad S(t) = \sum_n |c_n(t)|^2 \quad (7)$$

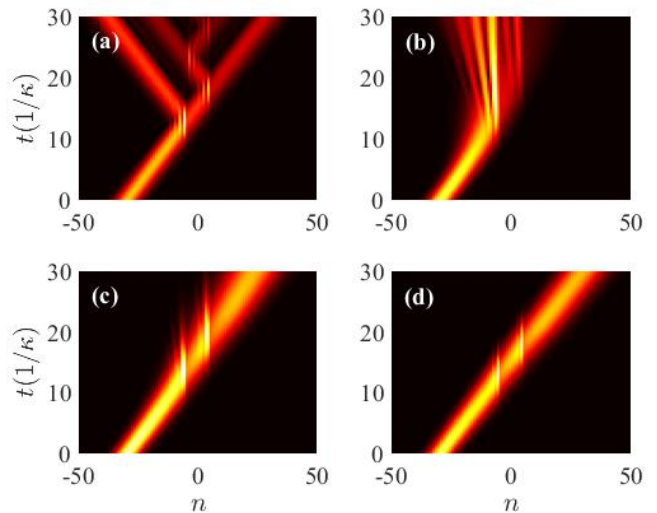


FIG. 4: (Color online) Dynamics of wave propagation in Hermitian and non-Hermitian lattices with Gaussian excitation at initial time. We plot in figures the space-time evolution of the normalized probability amplitude  $|\rho_n(t)|$  in Hermitian lattices [(a)] and non-Hermitian lattices [(b)-(d)] with defects. We set  $\gamma = \beta = 0$  in the Hermitian case and  $\beta = 0.4\kappa, \gamma = 0.8\kappa$  in the non-Hermitian case. The lattice defects are assumed to be  $V_c = 2\kappa$  at  $n = \pm 5$ . We assume here a Gaussian wave packet with  $n_0 = -30, w_0 = 5, q_0 = -\pi/2$ . Other parameters are (b)  $\phi = 0$ , (c)  $\phi = \pi/4$  and (d)  $\phi = \pi/2$ . In the Hermitian case the dynamics do not depend on the phase  $\phi$ .

Note a single-site excitation corresponds to an incident wave including components with all Bloch wave numbers in the first Brillouin zone. So for a general Hermitian lattice ( $\gamma = \beta = 0$ ), the incident light propagates with all velocities in the range  $[-2\kappa, 2\kappa]$ , as shown in Fig. 3 (a), an expanding sector-type propagation pattern arises instead of a beam-type pattern. However, for a non-Hermitian lattice with complex hopping rates, owing to the existence of the imaginary energy band, the incident wave propagates only with the velocity corresponds to  $\text{Im}(E) = 0$ . As shown in Fig. 3 (b)-(d), by adjusting the phase  $\phi$ , one can realize a transition between localization and delocalization of incident light and a control of group velocity. Physically, this is because the group velocity corresponds to  $\text{Im}(E) = 0$  is vanishing when  $\phi = 0$ , incident components with other wave numbers decay rapidly during propagation. By adjusting the phase  $\phi$ , the lossless incident component acquire a nonvanishing velocity. The group velocity tends to the maxima as  $\phi \rightarrow \pi/2$  according to Eq. (6). In addition, a left-propagating wave with similar behavior can also be achieved by adjusting  $\phi$  to be negative, according to Eq. (5).

A robust unidirectional photon transport can be exhibited in the non-Hermitian lattice by introducing lattice defects, i.e., additional potential terms such as  $V_{add} = V_c(\delta_{n,10} + \delta_{n,20})$  with  $V_c = 2\kappa$  in Fig. 3 (e) and (f). One can find in Fig. 3 (e) that the right-propagating wave in the Hermitian lattice undergoes multiple transmissions

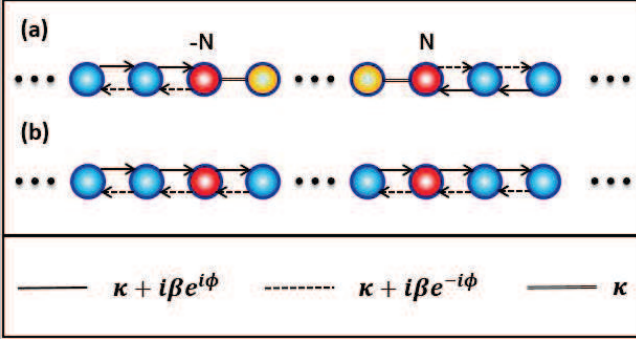


FIG. 5: (Color online) Schematic illustration of the photon storage process: (a) The three-stage heterogeneous structure used for photon capture and (b) defective homogeneous non-Hermitian lattice used for photon release. Blue and yellow circles indicate sites of the non-Hermitian and the Hermitian parts, respectively. Red circles indicate the boundary sites with defect  $V_c$ . The hopping rates of the two semi-infinite non-Hermitian parts in (a) are asymmetric due to the opposite synthetic magnetic fluxes, whereas they are symmetric in (b). The hopping rates of the Hermitian part in (a) are real and identical.

and reflections at the two defects and the wave attenuates rapidly after each scattering, whereas in Fig. 3 (f) the wave propagates robustly in the non-Hermitian lattice, immune to the defects. The physical reason thereof is as follows: In Hermitian lattices, the dispersion curve is the same as the real part of the non-Hermitian case in Fig. 2 but with a vanishing imaginary part. The energy is degenerate and there always exists a reflected wave with wave number  $q'$  satisfies  $q' = -q_0$  and  $E(q') = E(q_0)$ , where  $q_0$  is the incident wave number. It means that an elastic scattering from the defect is allowed in this case. However, in the non-Hermitian case, due to the existence of the imaginary dispersion curve, the energy becomes non-degenerate, there is no real wave numbers satisfy  $E(q') = E(q_0)$ , thus the elastic scattering and thereby the reflected waves are inhibited, a robust unidirectional photon transport arises.

The robustness of photon transport can also hold in the non-Hermitian lattice with a Gaussian excitation

$$c_n(0) \propto \exp\left[-\frac{(n - n_0)^2}{w_0^2} + iq_0 n\right] \quad (8)$$

where  $n_0$  and  $q_0$  are respectively the incident lattice site and the Bloch wave number of the incident wave, and  $w_0$  is the width of the Gaussian wave packet. Differing from single-site excitation, Gaussian wave packet contains only one Bloch wave number and propagates with a certain velocity. Similar to Fig. 3 (e), one can find in Fig. 4 (a) that the left incident wave in a Hermitian lattice is multiply scattered by the defects and the scattering waves decay rapidly. As a comparison, the behavior in a non-Hermitian lattice is shown in Fig. 4 (b)-(d), where the photon transport tends to be more and more robust as the phase  $\phi$  varies from 0 to  $\pi/2$ . Similar behaviors can

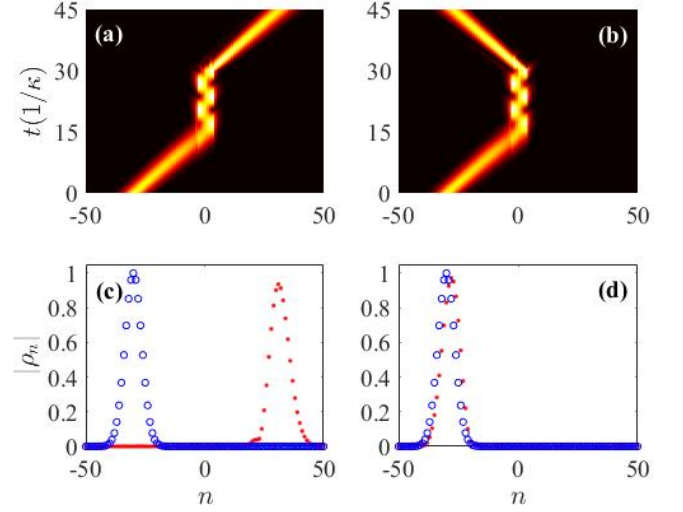


FIG. 6: (Color online) Storage and reversal of a left incident Gaussian wave packet in the three-stage heterogeneous structure. (a) Space-time evolution of photon storage process. (b) Space-time evolution of photon reversal process. (c) and (d) Normalized amplitude profile  $|\rho_n|$  versus the lattice sites  $n$  for storage and reversal processes, respectively. The Gaussian excitation we used here is the same as the one in Fig. 4. The switch time in (a) and (b) is  $t'\kappa = 30$ . The defects at the boundary sites  $n = \pm N$  are  $V_c = \kappa$  where  $N = 3$ . Other parameters in Eqs. (9) and (10) are the same as those in Fig. 4.

also arise for a right incident wave but with  $\phi \rightarrow -\phi$  in Eq. (4).

Physically, for a non-Hermitian lattice with  $\phi = 0$ , the dispersion curve is symmetric with respect to  $q = 0$  in the first Brillouin zone, similar to that in the Hermitian case but possesses an additional imaginary part. The degenerate energy allows elastic scattering and thereby reflections. Moreover, the incident wave number  $q_0 = -\pi/2$  corresponds to a damped propagation. Thus reflections and attenuation can be observed in Fig. 4 (b) like in a Hermitian lattice. As  $\phi \rightarrow \pi/2$ , according to Eq. (5), the imaginary part of the dispersion relation tends to be vanishing, illustrating a lossless propagation is achieved. The energy losses the degeneracy and thus reflections are inhibited. In view of this, robust unidirectional photon transport which is immune to defects and backscattering can be realized in the non-Hermitian lattice.

It is worth to note that Gaussian wave packets with other incident wave numbers can also propagate robustly by adjusting the phase to satisfy  $\phi = -q_0$ , according to Eq. (5). It is very different from Hermitian lattices and non-Hermitian lattices without phase-modulated imaginary parts. Furthermore, the Hermitian case in Fig. 4 (a) is similar to photon transport in a Fabry-Perot cavity. In view of this, lossless and robust photon transport can also be realized in cavity quantum electrodynamics (CQED) with complex hopping rates similar to that in this work.

#### IV. PHOTON STORAGE AND REVERSAL

Besides robust unidirectional transport, the non-Hermitian lattice can also be utilized as a photon storer. To achieve photon storage, we consider a system which can be switched between a sandwich (i.e., three-stage heterogeneous) structure and a defective homogeneous non-Hermitian lattice, as shown in Fig. 5. The sandwich structure is formed with a finite Hermitian lattice embedded between two semi-infinite non-Hermitian lattices, as shown in Fig. 5 (a). The phase (synthetic magnetic fluxes) of the two non-Hermitian parts which modulate the imaginary parts of the hopping rates are op-

posite, leading to two asymmetric non-Hermitian parts. There exist two identical defects  $V_c$  at the boundary sites  $n = \pm N$ . The Hermitian part can be realized by applying additional auxiliary sites for each site of the original non-Hermitian lattice in this area. By modulating the potentials of the additional auxiliary sites, one can acquire opposite imaginary hopping rates which can offset the original imaginary parts. We excite such a sandwich structure at initial time  $t = 0$  by a Gaussian wave packet with Bloch wave number  $q_0$ . For a left incident wave, we set the phase  $\phi = -q_0$ . Taking into account all the conditions above, the evolution equations of the system can be written as

$$i \frac{dc_n}{dt} = \begin{cases} -i\gamma c_n + (\kappa + i\beta e^{-iq_0})c_{n+1} + (\kappa + i\beta e^{iq_0})c_{n-1} & n < -N \\ (V_c + i\xi)c_n + \kappa c_{n+1} + (\kappa + i\beta e^{iq_0})c_{n-1} & n = -N \\ \kappa(c_{n+1} + c_{n-1}) & -N < n < N \\ (V_c + i\xi)c_n + (\kappa + i\beta e^{iq_0})c_{n+1} + \kappa c_{n-1} & n = N \\ -i\gamma c_n + (\kappa + i\beta e^{iq_0})c_{n+1} + (\kappa + i\beta e^{-iq_0})c_{n-1} & n > N \end{cases} \quad (9)$$

Note the sudden change of the dispersion relation at the boundary sites gives rise to an amplification or attenuation of the wave. According to Eq. (9), whenever the wave is reflected by the defects in the Hermitian area, the imaginary part of the dispersion relation of the boundary sites, i.e.,  $\text{Im}[E(Q)] = i\beta \cos(2q_0)$ , leads to an amplification or attenuation which depends on the value of  $q_0$ . The effect of the process is non-negligible due to the multiple reflections in the Hermitian area, as discussed in below. In view of this, we introduce additional imaginary potential  $i\xi$  for the boundary sites to offset the amplification or attenuation.

We set  $\xi = \beta$  in Fig. 6 due to the wave number of the Gaussian wave packet we used here is  $q_0 = -\pi/2$ . As shown in Fig. 6 (a), the left incident Gaussian wave packet propagates unidirectionally in the first non-Hermitian part, as discussed in the previous section. Once the incident wave enters into the Hermitian part, it is scattered back and forth between the two defects. The photons are thus captured in the Hermitian area. By adjusting potentials of the additional auxiliary sites and the relevant phase (to be identical over the whole lattice) at  $t = t'$  [ $(t'\kappa = 30)$  in Fig. 6], the system becomes a defective homogeneous non-Hermitian lattice as shown in Fig. 5 (b), i.e.,

$$i \frac{dc_n}{dt} = -i\gamma c_n + (\kappa + i\beta e^{i\phi})c_{n+1} + (\kappa + i\beta e^{-i\phi})c_{n-1} + V_c(\delta_{n,-N} + \delta_{n,N}) \quad (10)$$

one can find a retrieved wave propagates in the same direction with  $\phi = -q_0$ . We plot in Fig. 6 (c) the

normalized amplitude profiles of the incoming and outgoing waves. The outgoing wave keeps the Gaussian shape means the storage in this system is almost shape-preserving. Photon reversal can also be observed if the phase of the defective homogeneous non-Hermitian lattice satisfies  $\phi = q_0$  in Eq. (10), as shown in Fig. 6 (b). The wave propagates in the opposite direction after retrieval. We plot in Fig. 6 (d) the normalized amplitude profiles of the incoming and outgoing waves in this case and again we find an almost shape-preserving outgoing wave. Similar behaviors can also arise for a right incident wave but with  $q_0 \rightarrow -q_0$  in Eq. (9) and  $\phi \rightarrow -\phi$  in Eq. (10). Note that the storage time and the storage range (width of the Hermitian area) can be artificially controlled by adjusting the switch time  $t'$  and the boundary position  $N$  within limits, respectively. Similar scheme, i.e., realizing photon storage in a sandwich structure, has been proposed in an atomic system [31]. Where the incident light undergoes similar multiple reflections back and forth in the middle area of the system. In view of this, photon storage and reversal with controllable storage time and range can be realized in the non-Hermitian lattice.

The physical regime underlying is that, once the incident wave enters into the Hermitian part of the heterogeneous structure, it undergoes multiple reflections between the defects due to reflections are allowed in the Hermitian lattice as discussed above. Transmissions are inhibited because the energies correspond to  $q_0$  are asymmetry with respect to the boundary sites, i.e.,  $E(q_0) \neq E'(q_0)$ , where  $E$  and  $E'$  are energies of different areas. Thus the

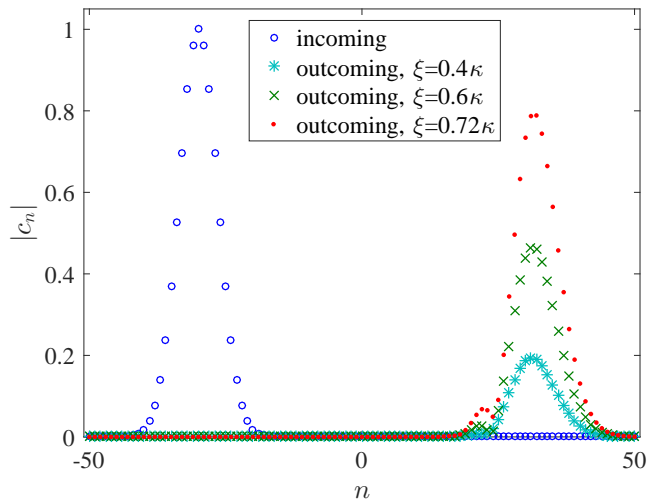


FIG. 7: (Color online) Profiles of the actual probability amplitude  $|c_n|$  of the incoming and outcoming waves with different offset coefficient  $\xi$  of the boundary sites. All the parameters except for  $\xi$  are the same as those in Fig. 6.

wave is reflected back and forth, localizing in the Hermitian area. Once the sandwich structure is switched to the defective homogeneous non-Hermitian lattice, due to the robustness of photon transport in such a lattice as discussed above, the defects can no longer prevent transmissions and thereby the wave is retrieved. Similar analysis also holds for a right incident wave.

In order to show the storage efficiency of the photon storage scheme, we plot in Fig. 7 the actual amplitude profiles of the incoming and outcoming waves in Fig. 6. One can find that the actual amplitude of the outcoming wave with  $\xi = \beta = 0.4\kappa$  is much weaker than the incoming one, although we have applied offset potential for the boundary sites. This is because the Bloch wave number of a Gaussian wave packet like Eq. (8) is not exactly  $q_0$  but a narrow range due to the width  $w_0$ . Thus the components of the Gaussian wave packet with wave numbers which are not exactly  $q_0$  undergo an attenuation during propagation. The multiple reflections in the Hermitian area give rise to a greatly increased propagation distance and thereby a increased attenuation. In spite of this, as in Fig. 7, one can increase the storage efficiency by enhancing the offset coefficient  $\xi$  of the boundary sites. With

an increasing  $\xi$ , the actual amplitudes of the outcoming waves enhance significantly, and the shape-preserving effect is satisfactory. Moreover, one can also increase the storage efficiency by applying gain effect for the finite sites in the Hermitian area. That is to say, the photon storage scheme can be optimized readily.

## V. CONCLUSIONS

In summary, we study a non-Hermitian lattice with complex hopping rates whose imaginary parts are modulated by an additional phase. Such a non-Hermitian lattice can be realized by a quasi-one-dimensional sawtooth-type Hermitian lattice, consisting of a main sublattice and an auxiliary sublattice. With proper conditions, the auxiliary sublattice can be eliminated adiabatically and thereby the complex hopping rates arise. With this lattice, robust and reflectionless unidirectional photon transport can be realized, in spite of the existence of defects on the lattice. By adjusting the phase, one can realize a switch between localization and delocalization for both single-site and Gaussian excitations. Furthermore, the non-Hermitian lattice can also be used for a photon storer. By modulating relevant parameters especially the phase, photon storage and reversal can be observed in the lattice. The storage time and range can be artificially controlled within limits which are rather difficult in other schemes. The storage efficiency can be increased by enhancing the gain effect of the boundary sites or the Hermitian sites. The main results in this paper, including the implementation scheme of the non-Hermitian lattice with modulated complex hopping rates, providing a promising platform for controllable photon transport. The proposal of photon storage and reversal also opens up a new path for quantum information process (QIP).

## ACKNOWLEDGMENTS

Thanks Dr. Yi-Mou Liu for helpful discussions and Dr. Chu-Hui Fan for constructive suggestions. This work is supported by National Natural Science Foundation of China (Grants No. 61378094, No. 10534002, No. 11674049, and 11704064).

[1] S. Lepri and G. Casati, Asymmetric wave propagation in nonlinear systems, *Phys. Rev. Lett.* **106**, 164101 (2011).  
 [2] J. D. Ambrose, P. G. Kevrekidis, and S. Lepri, Asymmetric wave propagation through nonlinear PT-symmetric oligomers, *J. Phys. A: Math. Theor.* **45**, 444012 (2012).  
 [3] U. Al Khawaja and A. A. Sukhorukov, Unidirectional flow of discrete solitons in waveguide arrays, *Opt. Lett.* **40**, 2719 (2015).

[4] M. Z. Hasan and C. L. Kane, Topological insulators, *Rev. Mod. Phys.* **82**, 3045 (2010).  
 [5] X.-L. Qi and S.-C. Zhang, Topological insulators and superconductors, *Rev. Mod. Phys.* **83**, 1057 (2011).  
 [6] L. Lu, J. D. Joannopoulos, and M. Soljacic, Topological photonics, *Nature Photon.* **8**, 821 (2014).  
 [7] N. Hatano and D. R. Nelson, Localization Transitions in NonHermitian Quantum Mechanics, *Phys. Rev. Lett.* **77**, 570 (1996).

- [8] N. Hatano and D. R. Nelson, Vortex pinning and non-Hermitian quantum mechanics, *Phys. Rev. B* **56**, 8651 (1997).
- [9] P. W. Brouwer, P. G. Silvestrov, and C. W. J. Beenakker, Theory of directed localization in one dimension, *Phys. Rev. B* **56**, R4333 (1997).
- [10] N. M. Shnerb and D. R. Nelson, Winding Numbers, Complex Currents, and Non-Hermitian Localization, *Phys. Rev. Lett.* **80**, 5172 (1998).
- [11] D. R. Nelson and N. M. Shnerb, Non-Hermitian localization and population biology, *Phys. Rev. E* **58**, 1383 (1998).
- [12] N. Hatano and D. R. Nelson, Non-Hermitian delocalization and eigenfunctions, *Phys. Rev. B* **58**, 8384 (1998).
- [13] I. V. Yurkevich and I. V. Lerner, Delocalization in an Open One-Dimensional Chain in an Imaginary Vector Potential, *Phys. Rev. Lett.* **82**, 5080 (1999).
- [14] T. Kuwae and N. Taniguchi, Two-dimensional non-Hermitian delocalization transition as a probe for the localization length, *Phys. Rev. B* **64**, 201321 (2001).
- [15] S. Longhi, Invisibility in non-Hermitian tight-binding lattices, *Phys. Rev. A* **82**, 032111 (2010).
- [16] M. S. Rudner and L. S. Levitov, Topological Transition in a Non-Hermitian Quantum Walk, *Phys. Rev. Lett.* **102**, 065703 (2009).
- [17] M. S. Rudner and L. S. Levitov, Phase transitions in dissipative quantum transport and mesoscopic nuclear spin pumping, *Phys. Rev. B* **82**, 155418 (2010).
- [18] J. M. Zeuner, M. C. Rechtsman, Y. Plotnik, Y. Lumer, S. Nolte, M. S. Rudner, M. Segev, and A. Szameit, Observation of a Topological Transition in the Bulk of a Non-Hermitian System, *Phys. Rev. Lett.* **115**, 040402 (2015).
- [19] F. Baboux, L. Ge, T. Jacqmin, M. Biondi, E. Galopin, A. Lemaître, L. Le Gratiet, I. Sagnes, S. Schmidt, H. E. Treci, A. Amo, and J. Bloch, Bosonic condensation and disorder-induced localization in a flat band, *Phys. Rev. Lett.* **116**, 066402 (2016).
- [20] H. Ramezani, Non-Hermiticity induced flat band, *Phys. Rev. A* **96**, 011802(R) (2017).
- [21] D. Leykam, S. Flach, and Y. D. Chong, Flat bands in lattices with non-Hermitian coupling, *Phys. Rev. B* **96**, 064305 (2017).
- [22] S. Longhi, Kramers-Kronig potentials for the discrete Schrödinger equation, *Phys. Rev. A* **96**, 042106 (2017).
- [23] S. Longhi, Reflectionless and invisible potentials in photonic lattices, *Opt. Lett.* **10**, 1364 (2017).
- [24] S. Longhi, D. Gatti, and G. D. Valle, Robust light transport in nonHermitian photonic lattices, *Sci. Rep.* **5**, 13376 (2015).
- [25] S. Longhi, D. Gatti, and G. D. Valle, Non-Hermitian transparency and one-way transport in low-dimensional lattices by an imaginary gauge field, *Phys. Rev. B* **92**, 094204 (2015).
- [26] S. Longhi, Non-Hermitian tight-binding network engineering, *Phys. Rev. A* **93**, 022102 (2016).
- [27] S. Longhi, Non-Hermitian bidirectional robust transport, *Phys. Rev. B* **95**, 014201 (2017).
- [28] L. Jin, P. Wang, and Z. Song, One-way light transport controlled by synthetic magnetic fluxes and  $\mathcal{PT}$ -symmetric resonators, *New J. Phys.* **19**, 015010 (2017).
- [29] M. Schmidt, S. Kessler, V. Peano, O. Painter, and F. Marquardt, Optomechanical creation of magnetic fields for photons on a lattice, *Optica* **2**, 635 (2015).
- [30] S. Longhi, Aharonov-Bohm photonic cages in waveguide and coupled resonator lattices by synthetic magnetic fields, *Optics Lett.* **39**, 5892 (2014).
- [31] J.-H. Wu, M. Artoni, and G. C. La Rocca, All-Optical Light Confinement in Dynamic Cavities in Cold Atoms, *Phys. Rev. Lett.* **103**, 133601 (2009).